

Observation of Collective Molecular Dynamics in a Chalcogenide Glass: Results from X-ray Photon Correlation Spectroscopy

Jianheng Li, Meera Madhavi, Spencer Jeppson, Louie Zhong, Eric M. Dufresne, Bruce Aitken, Sabyasachi Sen, and Roopali Kukreja*



Cite This: *J. Phys. Chem. B* 2022, 126, 5320–5325



Read Online

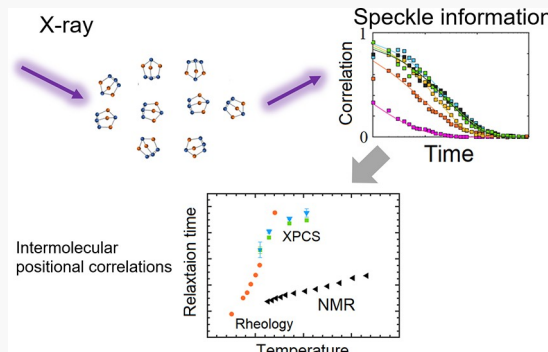
ACCESS |

Metrics & More

Article Recommendations

Supporting Information

ABSTRACT: The structural relaxation processes in a $\text{Ge}_3\text{As}_{52}\text{S}_{45}$ molecular chalcogenide glass sample were directly studied by X-ray photon correlation spectroscopy (XPCS). XPCS was conducted at the first sharp diffraction peak at $q = 1.16 \text{ \AA}^{-1}$ at temperatures ranging from 123 K to above the glass transition at 328 K, and the results showed two different dynamical regimes. At a low temperature, the observed glass dynamics are slow and dominated by X-ray-photon-induced effects, which are temperature independent. At a higher temperature, we observed a dramatic decrease in the fluctuation timescales, indicating that the dynamics were mainly due to the intermolecular correlation of the As_4S_3 molecule in the glass. The timescales in this high-temperature range agree well with those determined from measurements of the Newtonian viscosity. Our XPCS studies suggest an extended length scale of the relaxation process in glassy $\text{Ge}_3\text{As}_{52}\text{S}_{45}$ from the single molecule to the intermolecular range across the glass transition, providing a unique direct probe of the dynamics beyond the length scales of the individual molecule.



1. INTRODUCTION

The dynamics of the liquid-to-glass transition are extensively investigated phenomena as the question of a thermodynamic versus kinetic origin poses challenging and yet unsolved problems in the field of condensed matter physics and chemistry.¹ The shear relaxation in “fragile” supercooled liquids displays a remarkable slowdown as the temperature approaches the glass transition temperature (T_g) from above. For example, for the molecular liquid *ortho*-terphenyl, the shear relaxation timescale (τ_{shear}) increases by 10 orders of magnitude as temperature decreases by ~ 75 K.² Such a dynamical slowdown implies the existence of a growing or even diverging length scale of domains of correlated dynamics as the temperature approaches T_g upon cooling, which has been extensively corroborated by simulation studies.^{3–8} However, direct and unequivocal experimental observation of this dynamical lengthscale and its temperature dependence in supercooled glass-forming liquids has remained elusive. Understanding how shear relaxation is controlled by the dynamics that involve intermolecular positional correlations at different length scales holds the key in this regard.

Spectroscopic studies on organic molecular glass-forming liquids have indicated that the translational and rotational diffusion of the constituent molecules are intimately related to the shear and structural relaxation.^{9–11} On the other hand, we have reported in previous studies the finding of a large temporal decoupling in inorganic molecular liquids between

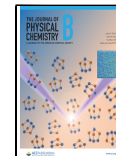
the timescale of isotropic self-rotation of the roughly spherical As_4S_3 and P_4Se_3 cage molecules and τ_{shear} by several orders of magnitude near T_g .^{12,13} Such a large decoupling may not be entirely surprising since the energetic barrier to rotational reorientation of molecules with a higher degree of sphericity is expected to be low, and therefore, such dynamics can be weakly coupled to the shear relaxation of the liquid. It is, therefore, tempting to argue that in these liquids the dynamics responsible for the shear relaxation may involve length scales that must go beyond the dimensions of single molecules and likely involve collective motion of multiple molecules, that is, intermolecular positional correlations. An investigation of this effect requires an experimental technique that can access both subnanometer spatial resolution and subsecond temporal resolution. In this article, we have utilized X-ray photon correlation spectroscopy (XPCS) to characterize the collective molecular dynamics in the chalcogenide glass of the composition $\text{Ge}_3\text{As}_{52}\text{S}_{45}$.

The structure of this chalcogenide glass has been shown in previous studies to consist of isolated cage-like As_4S_3 molecules

Received: December 3, 2021

Revised: April 29, 2022

Published: June 22, 2022



ACS Publications

© 2022 American Chemical Society

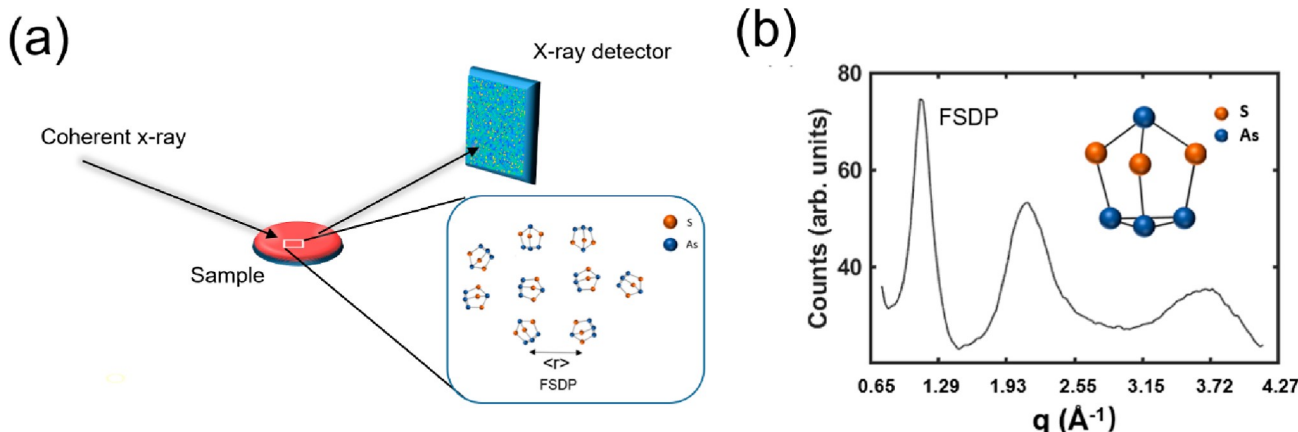


Figure 1. (a) Scattering geometry of the experiment and the schematic illustration of the molecular structure of this glass (Ge atoms are not shown), where As_4S_3 molecules are held together by van der Waals forces with an average intermolecular distance of $\langle r \rangle$. (b) X-ray scattering intensity obtained from the $\text{Ge}_3\text{As}_{52}\text{S}_{45}$ sample, with FSDP as labeled. The inset shows a schematic diagram of the As_4S_3 molecule.

that are held together by van der Waals forces, with $\text{Ge}_3\text{As}_{52}\text{S}_{45}$ being a representative composition.^{12,14} These molecules are cage-shaped, consisting of a 3-membered As_3 ring surmounted by an AsS_3 pyramid, with each S atom being bonded to an As atom in the As_3 ring that is directly below it. This glass, owing to its molecular nature, displays unusual physical properties, including a relatively high fragility index $m \sim 102$ where

$$m = \left. \frac{d(\log \tau_{\text{shear}})}{d\left(\frac{T_g}{T}\right)} \right|_{T=T_g}, \text{ low } T_g \text{ } (\sim 312 \text{ K}), \text{ and a high thermal}$$

expansion coefficient (96 ppm/K).¹⁴ The high degree of intermolecular As–As correlational ordering results in a strong first sharp diffraction peak (FSDP).^{15,16} The XPCS measurements reported here were performed by accessing the FSDP of this glass, which enabled us to investigate the molecular dynamics that involve the temporal decay of the intermolecular positional correlation of the constituent As_4S_3 molecules over a length scale of $\sim 5\text{--}6 \text{\AA}$. These measurements were carried out at temperatures ranging from 123 K to immediately above its T_g up to 328 K. We observed that X-ray-photon-induced dynamics dominate at low temperatures, while at higher temperatures near T_g , the intermolecular positional correlations play a stronger role. We observe that the X-ray-induced dynamics directly depend on the X-ray fluence and occur on a relatively slower timescale, while the collective molecular dynamics are faster and highly temperature-dependent. Near and above T_g , the timescale of the intermolecular correlational dynamics is found to be in good agreement with the τ_{shear} for this liquid.

2. EXPERIMENTAL SECTION

The $\text{Ge}_3\text{As}_{52}\text{S}_{45}$ glass was synthesized by melting a mixture of the starting elements ($\geq 99.9995\%$ purity in metals basis) in an evacuated (10^{-6} Torr) fused silica ampoule at a temperature of 1073 K in a rocking furnace for at least 24 h, and subsequently quenching the ampoule in cold water. The small amount of Ge doping (3 at %) was necessary in stabilizing this As-rich sulfide glass against devitrification. The recovered glass sample was cylindrical in shape and was cut into $\sim 1 \text{ mm}$ thick disks of diameter $\sim 5 \text{ mm}$.

The Newtonian viscosity of the $\text{Ge}_3\text{As}_{52}\text{S}_{45}$ liquid in the range $\sim 10^4\text{--}10^8 \text{ Pa}\cdot\text{s}$ was measured in a parallel plate rheometer (MCR 92, Anton-Paar) using steady shear in an

environment of flowing nitrogen gas. In this rheometer, the temperature was controlled by a Peltier heater. Before the rheometry measurements, the glass samples were heated above the softening point to reach a viscosity of $\sim 10^5 \text{ Pa}\cdot\text{s}$ and trimmed between the two plates (8 mm diameter, stainless steel) to form a sandwich-like geometry with a gap of $\sim 1 \text{ mm}$. At each desired measurement temperature, the samples were allowed to equilibrate for 5 min. Viscosity was determined as the ratio of stress and strain rate at various shear rates ranging between 0.01 and 1 s^{-1} at each temperature.

The XPCS experiment was conducted at Beamline 8-ID-E of the Advanced Photon Source (APS) at the Argonne National Laboratory. The X-ray beam (7.35 keV) was focused onto a spot size of $5 \mu\text{m}$ using Be compound refractive lenses according to a scheme described in Table 2 of Ref 17. The $\text{Ge}_3\text{As}_{52}\text{S}_{45}$ sample was placed under a vacuum of 10^{-3} torr under a beryllium dome and was fixed at a symmetric scattering geometry with 2θ of 18° to access the FSDP. Scattered X-ray photons from the sample were collected by a two-dimensional (2D) Lambda detector with a pixel size of $55 \mu\text{m}$ positioned 1 m away from the sample. The sample stage temperature was controlled by a resistivity heater and Lakeshore temperature controller with a precision of 0.01 K. The glass sample was allowed to thermally equilibrate for 30 min at each temperature step before the actual measurement. XPCS measurements were performed on the FSDP of the $\text{Ge}_3\text{As}_{52}\text{S}_{45}$ sample from a temperature range of 123 to 328 K ($T_g \sim 312 \text{ K}$). For each XPCS scan from 123 to 318 K, an exposure time of 0.1 s was utilized to access subsecond dynamics, and a total of 10,000 images were collected. The q range that is used for the calculation of the autocorrelation curve is approximately 0.04 \AA^{-1} in both q_x and q_z directions. For the XPCS scan at 328 K, a 0.015 s exposure time was used to capture faster dynamics. In order to study the X-ray-beam-induced effects, we performed measurements at three X-ray beam intensities, F_1 , $F_{0.5}$, and $F_{0.25}$, where F_1 corresponds to the full intensity of the X-ray beam at $7.25 \times 10^9 \text{ photons/s}$, and $F_{0.5}$ and $F_{0.25}$ correspond to 50% and 25% of the full intensity. After each measurement, the sample stage was moved either 10 μm in a horizontal direction or 20 μm in a vertical direction to avoid any accumulated X-ray effects.

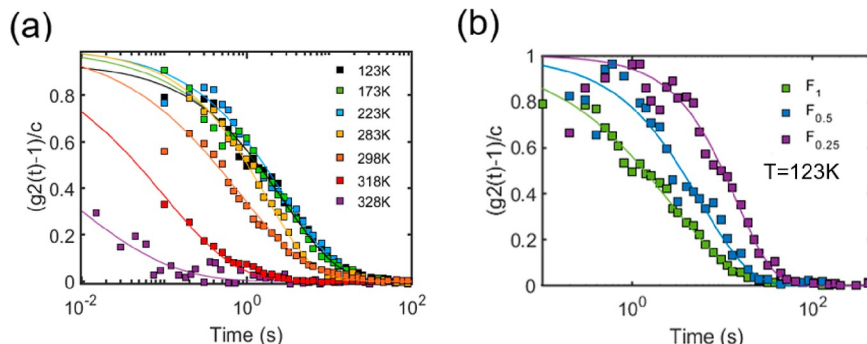


Figure 2. (a) Normalized g_2 autocorrelation curve for seven different temperatures at a beam fluence of F_1 . (b) Normalized g_2 autocorrelation curve for three different X-ray fluences, F_1 , $F_{0.5}$, and $F_{0.25}$, measured at a temperature of 123 K.

3. RESULTS

Figure 1b shows a θ – 2θ scan of the $\text{Ge}_3\text{As}_{52}\text{S}_{45}$ sample performed in a symmetric scattering geometry. The FSDP is located at $2\theta = 18^\circ$ or scattering wavevector $q = 1.16 \text{ \AA}^{-1}$, which corresponds to the intermolecular As–As correlation at $\sim 5.4 \text{ \AA}$.¹⁵ The scattering peaks observed at higher angles are the principal peak ($2\theta = 32^\circ$) that represents the chemical ordering in an amorphous structure at the extended range length scale, and the secondary peak ($2\theta = 58^\circ$) corresponds to the topological ordering occurring near $q = 5\pi/2r$, where r is the mean nearest-neighbor distance (Figure 1a). Previous empirical potential structure refinement studies revealed that the principal peak arises from S–S, As–S, and As–As nearest-neighbor correlations in the structure.¹⁵ A schematic for the molecular structure of this glass is presented in Figure 1.

In order to study the dynamical behavior as a function of temperature, XPCS studies were performed using coherent X-rays. As coherent X-rays scatter from the local structure in the sample, they undergo a constructive/destructive interference resulting in a “speckle” pattern on the detector. This speckle pattern is a fingerprint of the detailed sample structure in reciprocal space and was measured as a function of time at a given temperature to investigate dynamical fluctuations in the sample. In order to quantify the time-dependent behavior, the temporal intensity correlation of the speckle pattern measured at the FSDP was calculated using autocorrelation function, $g_2(Q, t)$

$$g_2(Q, t) = \frac{\langle I(Q, \tau)I(Q, t + \tau) \rangle}{\langle I(Q, \tau) \rangle^2} \quad (1)$$

where $I(Q, t)$ and $I(Q, t + \tau)$ are the intensity values of a specific pixel at a given time and scattering vector.^{16,18} A spatial averaging of all the pixels in the q -range of 0.04 \AA^{-1} (for both q_x and q_z directions) for the FSDP was applied to obtain the g_2 function. The calculated autocorrelation was fitted with an empirical Kohlrausch–Williams–Watts-type stretched (or compressed) exponential function

$$g_2(Q, t) = 1 + C|F(Q, t)|^2 = 1 + c \text{e}^{-(t/\tau)^\beta} \quad (2)$$

where C is the speckle contrast factor, which is dependent on the experimental setup, background strength, and sample behavior; τ is the characteristic decay constant; β is the stretching (compression) exponent that controls the shape of the curve. The contrast values for all the measurements in this study range from 0.017 to 0.04 with no obvious temperature or X-ray fluence dependency (see the Supporting Information

section S1). For all the temperatures and X-ray fluences, $\beta < 1$ was obtained (see the Supporting Information section S4), which is indicative of glassy dynamics and has been previously observed in colloidal systems and glasses.

At the beginning of each XPCS scan, a decay of FSDP intensity is observed when the X-ray photon is first incident on the sample. The decay in intensity stabilizes within ~ 200 – 300 s with a maximum drop in amplitude of 10% of the initial value. Detailed analysis can be found in the Supporting Information S2, where this initial intensity stabilization can be treated as a nonequilibrium dynamical response, and the dynamics measured after 400 s correspond to steady-state fluctuations since no intensity change is observed for $t \geq 400$ s. For the rest of the data analysis and discussion in this article, we focus on the steady-state fluctuations observed during 400 s $\leq t \leq 1000$ s.

Figure 2a,b presents the g_2 curves that are normalized by contrast c , that is, $[g_2(t) - 1]/c$, as a function of temperature and fluence, respectively. It may be noted here that the square root of this function is equivalent to the intermediate scattering function. Figure 2a shows the temperature dependence of this function over a temperature range of 123–328 K for a fixed X-ray fluence F_1 , while Figure 2b shows the dependence on X-ray fluence (F_1 , $F_{0.25}$, $F_{0.5}$) at a temperature of 123 K. Fluence dependence at other temperatures can be found in section S3. Based on Figure 2a, we can divide the temperature behavior into a low-temperature regime and a high-temperature regime. In the low-temperature regime from 123 to 223 K, the normalized g_2 curves (referred as g_2 curves hereafter) almost overlap each other, suggesting a minimal dependence on the temperature. In the high-temperature regime from 283 to 328 K, where the temperature approaches T_g , the g_2 curves decay at a faster rate. At the highest temperature (328 K), the g_2 curve decays to zero within ~ 0.1 s. The difference in the temperature-dependent behavior of g_2 in these two regimes clearly indicates the presence of two separate dynamic processes. At lower temperatures in the range of 123–223 K, the equilibrium fluctuations of the glass are frozen-in at the timescale of the experimental observation, and the dynamics are predominantly driven by the X-ray beam, resulting in a nearly temperature-independent decay of g_2 . This is also clear from Figure 2b, where for 123 K, we see a strong dependence of the decay of g_2 on the incoming X-ray fluence. The high X-ray fluence at F_1 promotes the fastest decay of g_2 , followed by $F_{0.5}$. At an X-ray fluence of $F_{0.25}$, the decay of g_2 is the slowest for a given temperature, and this behavior is consistent at all measurement temperatures. As the temperature approaches T_g , both structural relaxation processes and X-ray-beam-induced

dynamics occur in the sample within the time window of observation. At 328 K, the g_2 curves for F_1 and $F_{0.5}$ overlap with each other, suggesting a minimal role of beam-induced dynamics at this temperature (Supporting Information S3).

In Figure 3, we plot τ , as obtained from fitting eq 2 to the $g_2(t)$, as a function of temperature and fluence. The parameter

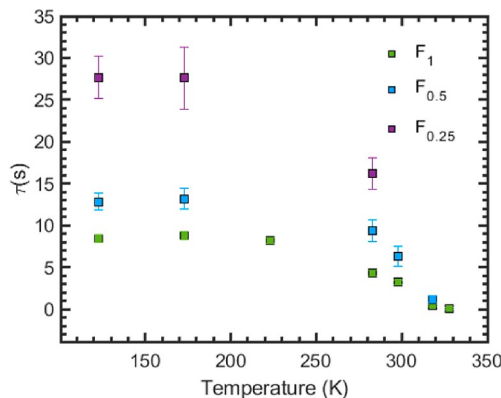


Figure 3. Characteristic decay time extracted by fitting eq 2 to the g_2 curves in Figure 2 as a function of temperature. At lower temperatures, there is no obvious temperature dependence on the fitted timescale but there is dependence on X-ray beam fluence, where a higher X-ray fluence promotes faster dynamics. At temperatures that are close or/and above T_g , we can observe a speeding up of the measured dynamics mainly due to the active intermolecular correlations as discussed in the text. Please note, at 328 K, the data points of F_1 and $F_{0.5}$ overlap well with each other.

τ describes the ensemble-averaged timescale governing molecular correlations and fluctuations in the $\text{Ge}_3\text{As}_{52}\text{S}_{45}$ system. At low temperatures in the range 123–223 K, τ is nearly independent of temperature but depends only on the X-ray fluence, which clearly highlights that the dynamics observed at these temperatures are induced by the X-ray beam. On the other hand, in the high-temperature regime ($T \geq 283$ K), τ decreases, and thus the dynamics become faster with increasing temperature. At 328 K, τ becomes independent of X-ray fluence and ranges around 0.05 s. These τ values are consistent with t_{shear} for this glass/supercooled liquid at this temperature as discussed below.

4. DISCUSSION

A deconvolution of the X-ray-beam-induced effects and equilibrium structural fluctuations in intermolecular correlations is needed for a meaningful analysis of the dynamics observed in the $\text{Ge}_3\text{As}_{52}\text{S}_{45}$ glass. As noted above, the exposure of the sample to the X-ray beam leads to a transient stage followed by steady-state fluctuations. In this steady-state regime, the observed dynamics in the temperature range 123–223 K can be attributed to purely beam-induced effects. The observation of such beam-induced dynamics in oxide glasses has been reported in recent studies by Ruta and co-workers.¹⁹ Moreover, the expected structural relaxation timescale in this temperature range well below T_g would be too long to observe within the time window of these measurements. In contrast, for higher temperatures (283–328 K), accelerated fluctuations are observed. In this regime, the equilibrium structural fluctuations associated with the collective motion of the constituent molecules start to contribute significantly to the estimated $\langle \tau \rangle$. However, as

illustrated in Figure 3, a contribution to $\langle \tau \rangle$ from beam-induced effects cannot be completely neglected at 283, 298, and 318 K although this contribution rapidly decreases with an increasing temperature and nearly vanishes at ~ 318 and 328 K.

A deconvolution model by Pintori et al. for the B_2O_3 glass has been previously proposed to separate structural relaxation and beam-induced dynamics, with the assumption that the beam-induced timescale is strictly temperature-independent even at T_g . The temperature independence was then utilized to estimate the two different timescales using, $\frac{1}{\tau_0} = \frac{1}{\tau_s} + \frac{1}{\tau_{\text{ind}}}$ where τ_0 is the fitted decay constant to the experimental g_2 curve, τ_{ind} is the timescale of the beam-induced dynamics that are temperature-independent, and τ_s is the structural relaxation timescale.²⁰ Based on the calculation shown in Table S5 in the Supporting Information, this model does not completely agree quantitatively with our measurements, implying that for the $\text{Ge}_3\text{As}_{52}\text{S}_{45}$ chalcogenide glass system, the mathematical deconvolution model may not be tenable. At lower temperatures, where the structural relaxation is too slow to be observed within the experimental time window, the X-ray-beam-induced dynamics control the decay of $g_2(t)$. However, with increasing temperature, both X-ray beam and structural relaxation actively promote molecular dynamics.

As the temperature increases, at $T \sim 318$ K, the estimated $\langle \tau \rangle$ becomes nearly independent of the X-ray fluence as shown in Figure 3. Finally, at $T \sim 328$ K, the estimated $\langle \tau \rangle$ is fully independent of the X-ray fluence and thus represents the true structural relaxation timescale. For both of these temperatures, we compare the $\langle \tau \rangle$ of ~ 0.4 – 1.3 s at 318 K and ~ 0.05 s at 328 K to the timescales of enthalpy and shear relaxation τ_{en} and τ_{shear} , respectively, near and above T_g (~ 312 K) in this system. Since T_g of this glass was determined using differential scanning calorimetry at a heating rate of 10 K/min, τ_{en} is estimated to be on the order of ~ 100 s at $T \sim T_g$.^{21,22} On the other hand, a recent study on supercooled liquids in the As–Se system has revealed that τ_{shear} for fragile glass-forming liquids can be significantly lower (e.g., an order of magnitude) than τ_{en} .²¹ We estimated τ_{shear} for this liquid from the viscosity data measured by parallel plate rheometry using the Maxwell relation $\tau_{\text{shear}} = \eta/G_{\infty}$, where η is the Newtonian viscosity, and G_{∞} is the glassy modulus, which for a wide variety of chalcogenide glasses is on the order of 5 GPa.

Figure 4 compares τ_{shear} with the decay constant $\langle \tau \rangle$ observed in our study using XPCS in the high-temperature regime. It can be clearly seen in Figure 4 that $\langle \tau \rangle$ indeed agrees well with τ_{shear} at 318 and 328 K. Since $\langle \tau \rangle$ from XPCS represents the timescale of a structural relaxation process that involves intermolecular correlations over a length scale of ~ 5 – 6 Å, the observed agreement between $\langle \tau \rangle$ and τ_{shear} points toward a temporal coupling between this relaxation process and the viscous flow at $T \geq 318$ K. In contrast, the self-rotation timescale of the constituent molecules in this liquid, as determined in a previous study by NMR spectroscopy,¹² couples to τ_{shear} only at significantly higher temperatures ($T > \sim 360$ K). Therefore, when taken together, these results clearly suggest that, compared to the single-molecule motion, a collective motion of molecules involving correlations at longer length scales becomes increasingly important for shear relaxation as the temperature approaches T_g from above in this fragile glass-forming liquid.

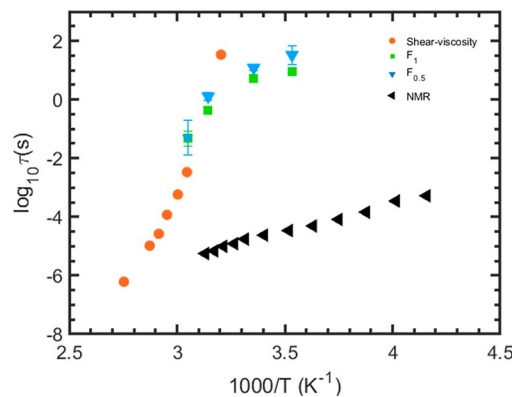


Figure 4. Characteristic decay time extracted from the g_2 curve at X-ray fluence of F_1 and $F_{0.5}$ measured at three temperatures close to T_g (green squares and blue inverted triangles). Orange circles represent τ_{shear} obtained from the viscosity data using the Maxwell relation (see the text for details).¹² Viscosity at calorimetric T_g is taken to be equal to its conventional value of 10^{12} Pa·s. Black triangles denote the self-rotation timescale of the constituent molecules measured in a previous study by NMR spectroscopy.¹²

5. CONCLUSIONS

In conclusion, XPCS measurements of molecular dynamics in the $\text{Ge}_3\text{As}_{52}\text{S}_{45}$ chalcogenide glass were performed from cryogenic temperatures (123 K) to just above its T_g by accessing the FSDP. The interaction of the X-ray photons with largely unconstrained As_4S_3 molecules results in a complex dynamical behavior. At low temperatures in the range of 123–223 K, a temperature-independent beam-induced dynamics are observed, which is attributed to the effect of energy transfer from X-ray photons to the sample. At higher temperature closer to T_g in the range of 283–328 K, the dynamics become dominated by the fluctuations in intermolecular correlations at a length scale of ~ 5 –6 Å, with timescales similar to τ_{shear} as obtained from the Newtonian viscosity. On the other hand, the single-molecule rotational correlation times at these temperatures are known to be orders of magnitude faster than τ_{shear} . These findings indicate that in this fragile glass-forming liquid, the molecular correlations at longer length scales become increasingly relevant for shear relaxation and viscous flow upon cooling toward the glass transition.

■ ASSOCIATED CONTENT

SI Supporting Information

The Supporting Information is available free of charge at <https://pubs.acs.org/doi/10.1021/acs.jpcb.1c10267>.

Contrast obtained from the XPCS measurements, initial intensity decay during X-ray exposure, fluence-dependent scans for all the measured temperatures, beta values obtained from fitting eq 2 to the g_2 autocorrelation function, deconvolution of beam-induced and glass dynamics timescales (PDF)

■ AUTHOR INFORMATION

Corresponding Author

Roopali Kukreja — Department of Materials Science and Engineering, University of California Davis, Davis, California 95616, United States; Email: rkkukreja@ucdavis.edu

Authors

Jianheng Li — Department of Materials Science and Engineering, University of California Davis, Davis, California 95616, United States; orcid.org/0000-0001-8212-7846

Meera Madhavi — Department of Materials Science and Engineering, University of California Davis, Davis, California 95616, United States; orcid.org/0000-0002-9726-9166

Spencer Jeppson — Department of Materials Science and Engineering, University of California Davis, Davis, California 95616, United States

Louie Zhong — Department of Materials Science and Engineering, University of California Davis, Davis, California 95616, United States

Eric M. Dufresne — Advanced Photon Source, Argonne National Laboratory, Lemont, Illinois 60439, United States

Bruce Aitken — Science & Technology Division, Corning Inc., Corning, New York 14831, United States

Sabyasachi Sen — Department of Materials Science and Engineering, University of California Davis, Davis, California 95616, United States; orcid.org/0000-0002-4504-3632

Complete contact information is available at:

<https://pubs.acs.org/10.1021/acs.jpcb.1c10267>

Notes

The authors declare no competing financial interest.

■ ACKNOWLEDGMENTS

J.L., M.M., S.J., L.Z., and R.K. would like to acknowledge the support from the Office of Naval Research (ONR grant no. N00014-19-1-2074). S.S. acknowledges the support from the National Science Foundation grant NSF-DMR 1855176. This research used resources of the Advanced Photon Source, a U.S. Department of Energy (DOE) Office of Science user facility operated for the DOE Office of Science by Argonne National Laboratory under contract no. DE-AC02-06CH11357.

■ REFERENCES

- 1) Cavagna, A. Supercooled Liquids for Pedestrians. *Phys. Rep.* **2009**, *476*, 51–124.
- 2) Eastwood, M. P.; Chitra, T.; Jumper, J. M.; Palmo, K.; Pan, A. C.; Shaw, D. E. Rotational Relaxation in ortho-Terphenyl: Using Atomistic Simulations to Bridge Theory and Experiment. *J. Phys. Chem. B* **2013**, *117*, 12898–12907.
- 3) Razul, M. S. G.; Matharoo, G. S.; Poole, P. H. Spatial Correlation of the Dynamic Propensity of a Glass-Forming Liquid. *J. Phys.: Condens. Matter* **2011**, *23*, 235103.
- 4) Chandler, D.; Garrahan, J. P. Dynamics on the Way to Forming Glass: Bubbles in Space-Time. *Annu. Rev. Phys. Chem.* **2010**, *61*, 191–217.
- 5) *Dynamical Heterogeneities in Glasses, Colloids, and Granular Media*; Berthier, L., Biroli, G., Bouchaud, J. P., Cipelletti, L., van Saarloos, W., Eds.; Oxford University Press: USA, 2011.
- 6) Karmakar, S.; Dasgupta, C.; Sastry, S. Growing Length and Time Scales in Glass-Forming Liquids. *Proc. Natl. Acad. Sci. U.S.A.* **2009**, *106*, 3675–3679.
- 7) Kim, K.; Saito, S. Multiple Length and Time Scales of Dynamic Heterogeneities in Model Glass-Forming Liquids: A Systematic Analysis of Multi-Point and Multi-Time Correlations. *J. Chem. Phys.* **2013**, *138*, 12A506.
- 8) Berthier, L.; Biroli, G. Theoretical Perspective on the Glass Transition and Amorphous Materials. *Rev. Mod. Phys.* **2011**, *83*, 587–645.
- 9) Swallen, S. F.; Bonvallet, P.A.; McMahon, R.J.; Ediger, M.D. Self-Diffusion of tris-Naphthylbenzene near the Glass Transition Temperature. *Phys. Rev. Lett.* **2003**, *90*, 015901.

(10) Ediger, M. D. Spatially Heterogeneous Dynamics in Supercooled Liquids. *Annu. Rev. Phys. Chem.* **2000**, *51*, 99–128.

(11) Fujara, F.; Geil, B.; Sillescu, H.; Fleischer, G. Translational and rotational diffusion in supercooled orthoterphenyl close to the glass transition. *Z. Phys. B* **1992**, *88*, 195–204.

(12) Gjersing, E. L.; Sen, S.; Yu, P.; Aitken, B. G. Anomalously Large Decoupling of Rotational and Shear Relaxation in a Molecular Glass. *Phys. Rev. B: Condens. Matter Mater. Phys.* **2007**, *76*, 214202.

(13) Kaseman, D. C.; Gulbiten, O.; Aitken, B. G.; Sen, S. Isotropic Rotation vs. Shear Relaxation in Supercooled Liquids with Globular Cage Molecules. *J. Chem. Phys.* **2016**, *144*, 174501.

(14) Aitken, B. G. GeAs Sulfide Glasses with Unusually Low Network Connectivity. *J. Non-Cryst. Solids* **2004**, *345*–346, 1–6.

(15) Kalkan, B.; Benmore, C. J.; Aitken, B. G.; Sen, S.; Clark, S. M. A Comparative Study of the Atomic Structures of Ge-Doped As_4S_3 and P_4Se_3 Molecular Glasses. *J. Non-Cryst. Solids* **2019**, *514*, 83–89.

(16) Nogales, A.; Fluerau, A. X Ray Photon Correlation Spectroscopy for the Study of Polymer Dynamics. *Eur. Polym. J.* **2016**, *81*, 494.

(17) Dufresne, E. M.; Narayanan, S.; Reininger, R.; Sandy, A. R.; Lurio, L. Focusing a round coherent beam by spatial filtering the horizontal source. *J. Synchrotron Rad.* **2020**, *27*, 1528–1538.

(18) Shpyrko, O. G. X-ray Photon Correlation Spectroscopy. *J. Synchrotron Radiat.* **2014**, *21*, 1057.

(19) Ruta, B.; Zontone, F.; Chushkin, Y.; Baldi, G.; Pintori, G.; Monaco, G.; Rufflé, B.; Kob, W. Hard X-rays as Pump and Probe of Atomic Motion in Oxide Glasses. *Sci. Rep.* **2017**, *7*, 3962.

(20) Pintori, G.; Baldi, G.; Ruta, B.; Monaco, G. Relaxation Dynamics Induced in Glasses by Absorption of Hard X-ray Photons. *Phys. Rev. B* **2019**, *99*, 224206.

(21) Xia, Y.; Yuan, B.; Gulbiten, O.; Aitken, B.; Sen, S. Kinetic and Calorimetric Fragility of Chalcogenide Glass-Forming Liquids: Role of Shear vs Enthalpy Relaxation. *J. Phys. Chem. B* **2021**, *125*, 2754–2760.

(22) Schawe, J. E. K. Vitrification in a Wide Cooling Rate Range: The Relations Between Cooling Rate, Relaxation Time, Transition Width, and Fragility. *J. Chem. Phys.* **2014**, *141*, 184905.

□ Recommended by ACS

Tailoring Phosphonium Ionic Liquids for a Liquid–Liquid Phase Transition

Beibei Yao, Zaneta Wojnarowska, *et al.*

MARCH 20, 2023

THE JOURNAL OF PHYSICAL CHEMISTRY LETTERS

READ 

Analysis of Structural Development and Defects during the Anisotropic Growth of Silicon

Lianxin Li and Tinghong Gao

OCTOBER 17, 2022

THE JOURNAL OF PHYSICAL CHEMISTRY B

READ 

Dynamics of Dendritic Ice Freezing in Confinement

James M. Campbell, Knut Jørgen Måloøy, *et al.*

MARCH 14, 2022

CRYSTAL GROWTH & DESIGN

READ 

How to Measure Hot Electron and Phonon Temperatures with Time Domain Thermoreflectance Spectroscopy?

Stéphane Grauby, Stefan Dilhaire, *et al.*

OCTOBER 31, 2022

ACS PHOTONICS

READ 

Get More Suggestions >